

Article

Determining the Relevance of Commonly Used Hydraulic Parameters for Representing the Water Erosive Force in Rock Mass Erosion within Dam Spillways

Aboubacar Sidiki Koulibaly ^{1,*} , Ali Saeidi ¹ , Alain Rouleau ¹  and Marco Quirion ²

¹ Department of Applied Sciences, University du Quebec at Chicoutimi, 555 Boulevard de l'Université, Chicoutimi, QC G7H 2B1, Canada; ali_saeidi@uqac.ca (A.S.); alain_rouleau@uqac.ca (A.R.)

² Dam Production and Expertise Unit, Hydro-Québec, 75 Boulevard René-Lévesque Ouest, Montréal, QC H2Z 1A4, Canada; quirion.marco@hydro.qc.ca

* Correspondence: aboubacar-sidiki.koulibaly1@uqac.ca; Tel.: +1-581-235-1247

Abstract: Spillways are essential control structures in hydroelectric dams for evacuating excess water during periods of high-water flow. These structures are generally excavated within a rock mass, without lining, and they take the form of a flow channel or a plunge pool. Rock mass erosion is an important issue facing engineers when designing unlined spillways. Methods commonly used to analyze this phenomenon are based on the threshold line concept, i.e., the correlation between rock mass resistance and its destruction against the erosive force of water. Multiple indices have been proposed for both rock mass quality and water energy (or erosive force) to assess rock mass erosion. The selection of appropriate indices is critical when evaluating hydraulic erosion. The erosive force of water is often represented by energy dissipation; however, other parameters, including average flow velocity and shear stress at the bottom of the flow channel, may also be relevant. Thus, a critical question is framed: which index best represents the erosive force of water? Here, we develop an approach to assess the applicability of the various indices used to represent the erosive force of water by relying on erosional events at more than 100 study sites. We determine that the most relevant parameters are linked to water pressure, as pressure head and flow velocity better explain the erosive force of the water than shear stress and water dissipation energy.

Keywords: energy dissipation; erosion class; hydraulic erosion; Kirsten index; rock mass; shear stress; water erosive force



Citation: Koulibaly, A.S.; Saeidi, A.; Rouleau, A.; Quirion, M. Determining the Relevance of Commonly Used Hydraulic Parameters for Representing the Water Erosive Force in Rock Mass Erosion within Dam Spillways. *Water* **2024**, *16*, 1261. <https://doi.org/10.3390/w16091261>

Academic Editors: Chengcheng Xia and Jian Luo

Received: 1 April 2024
Revised: 17 April 2024
Accepted: 24 April 2024
Published: 28 April 2024



Copyright: © 2024 by the authors. Licensee MDPI, Basel, Switzerland. This article is an open access article distributed under the terms and conditions of the Creative Commons Attribution (CC BY) license (<https://creativecommons.org/licenses/by/4.0/>).

1. Introduction

The potential for the erosion of rock mass within an unlined spillway is determined by comparing the resistance of the rock mass with the erosive force of flowing water. That erosion in dam spillways poses a constant threat to the safety of both individuals and equipment. Instances of unexpected erosion have led to serious damage to numerous dam spillways, resulting in substantial maintenance expenses for several large dams. For example, the Oroville Dam in California experienced significant damage due to a large cavity in its concrete spillway, resulting from a substantial water discharge that caused over USD 2 million in damages and necessitated the evacuation of downstream residents [1,2]. Similarly, at the 113 m high Copeton embankment dam in Australia, significant water flow in the bedrock spillway created a 20 m deep gorge [3]. To address this phenomenon, numerous studies involving laboratory tests using scaled-down physical models have been conducted. These physical models were designed to investigate the hydraulic characteristics of flows, assess erosion phenomena in granular materials or rock masses, and validate hypotheses used in the development of certain methods for predicting the erosion potential of rock mass within spillways. One subset of these models included the impact of hydraulic parameters on the erosion process, such as the slope of the flow

channel, flow rate, flow velocity, and surface roughness of the flow channel [4–8]. Moreover, some of these models focused on hydraulic parameters, aiming to simulate water flow or erosion downstream of weirs under specific conditions or to identify alternative solutions to reduce hydraulic power downstream of spillways [9–11]. Other models sought to investigate the effects of specific geomechanical parameters of the rock mass on hydraulic erosion [12–18].

Mostly based on the findings of these laboratory studies, several methods have been proposed to assess the potential risk of hydraulic erosion of a rock mass in dam spillways. These approaches are generally empirical, and all have limitations. Rock mass resistance is assessed through various indices of rock mass quality, whereas the erosive force of water is commonly represented by energy dissipation (Table 1).

Table 1. Existing methods for evaluating hydraulic erosion within dam spillways.

Method		Correlation Parameters	
Reference	Type	Erosive Force	Resistance of the Rock Mass
Moore [19], Van Schalkwyk [20], Annandale [21], Kirsten [22]	Empirical methods	Energy dissipation (Π_{UD} in $\text{kW}\cdot\text{m}^{-2}$)	Kirsten’s index (K)
Pells [3,23]			Geological strength index for erodibility ($eGSI$) Erodibility index of the rock mass ($RMEI_B$)

Rock mass resistance can be assessed by the Kirsten index (K), the geological strength index for erodibility ($eGSI$), and the rock mass erodibility index ($RMEI_B$), which all estimate rock mass quality. These indices use various geomechanical parameters related to the rock mass and the intact rock, such as the confined compressive strength of the intact rock (M_s), the size (K_b) or volume (V_b in m^3) of the rock blocks, the shear strength of the rock joints (K_d), and the relative structure of the blocks (either J_s or E_{doa}); the latter considers the effect of the shape and orientation of the blocks with respect to the flow direction of water in the channel. The values of K , $eGSI$, and $RMEI_B$ are determined using Equations (1), (2) and (3), respectively.

$$K = M_s \cdot K_b \cdot K_d \cdot J_s, \tag{1}$$

$$eGSI = GSI + E_{doa}, \tag{2}$$

$$RMEI_B = (RF_{P1} \cdot LF_{P1}) \cdot (RF_{P2} \cdot LF_{P2}) \cdot [(RF_{P3} \cdot LF_{P3}) + (RF_{P4} \cdot LF_{P4}) + (RF_{P5} \cdot LF_{P5})]. \tag{3}$$

GSI (Equation (2)) is a rock mass classification index developed by Hoek et al. [24]; it is also used by Pells as the basis for the $eGSI$ erodibility index. $RMEI_B$ (Equation (3)) defines the resistance of the rock mass by weighting the various geomechanical parameters using factors of relative importance (RF) and likelihood (LF). The prefixes $P1$ to $P5$ in Equation (3) represent various sets of geomechanical parameters, including the viable mechanisms at the kinematic separation of the blocks, the nature of the potentially eroded surface, the nature of the joints contained in the rock mass, joint spacing, and block shape [3].

Energy dissipation (Π_{UD}), which is favored in erosion-evaluation methods, is controlled by various parameters related to flow conditions. In the case of unlined spillway flow channels, Π_{UD} is determined using Equation (4) [23].

$$\Pi_{UD} = \rho \cdot g \cdot q \frac{dE}{dx'} \tag{4}$$

where ρ is the density of water ($\text{kg}\cdot\text{m}^{-3}$), g is the gravitational acceleration ($\text{m}\cdot\text{s}^{-2}$), q is the flow rate per unit length of channel width ($q = Q/B_f$), B_f is the channel width (m), Q is the water flow rate ($\text{m}^3\cdot\text{s}^{-1}$), and dE/dx is the energy loss during flow.

By combining the use of a rock mass resistance index with an index representing energy dissipation (Π_{UD} vs. K , Π_{UD} vs. $eGSI$, and Π_{UD} vs. $RMEI_B$), graphic methods can assess the erosion potential (Figure 1). Each point on these graphs represents a case of erosion that is categorized into damage classes on the basis of field observations, represented by using different symbols in various colors. These cases of erosion are also separated by theoretical damage classes represented by thresholds established through various methods, and these limits between the classes (and their number) can vary among authors. The Van Schalkwyk method includes three classes of erosion damage (Figure 1a) [20], Annandale’s has two damage classes (Figure 1b) [21], and Pells’ methods rely on five classes (Figure 1c,d) [3,23].

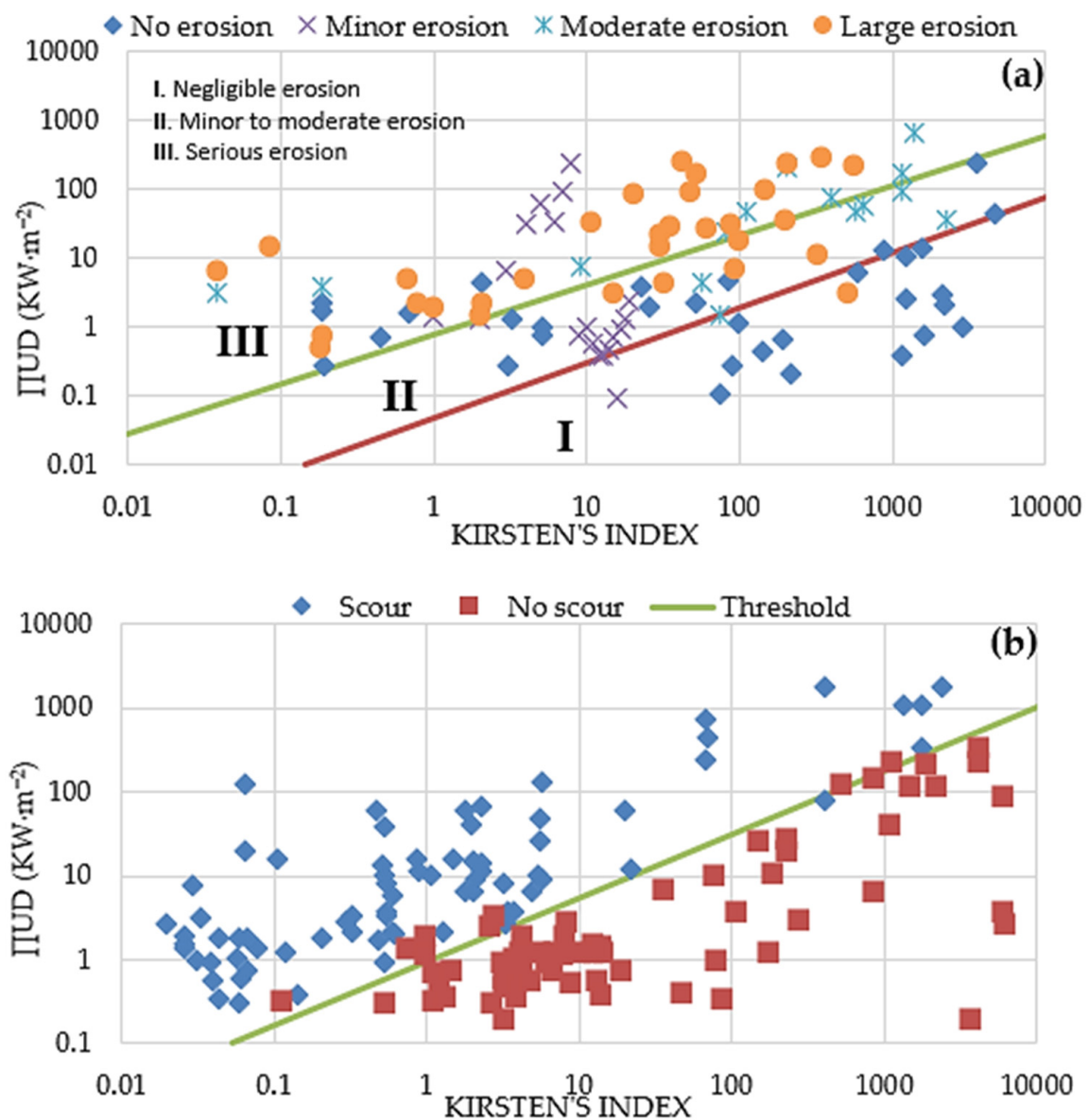


Figure 1. Cont.

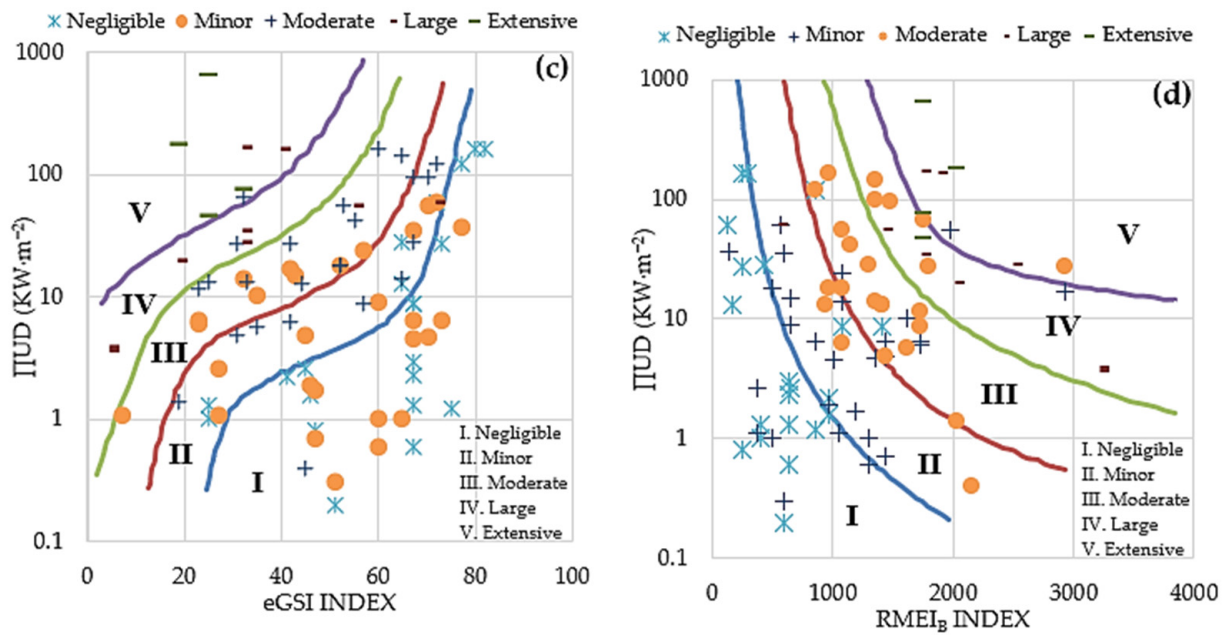


Figure 1. Methods for evaluating the hydraulic erodibility of rock mass in the flow channels of spillways, presenting the methods developed by (a) Van Schalkwyk et al. [20], (b) Annandale [21], and (c,d) Pells et al. [3,23].

A major inconsistency is apparent between the different damage classes (Figure 1). A common inconsistency for all existing methods is that the erosion class from field observations differs from that of the erosion evaluation methods (threshold lines). For example, a large portion of the “negligible” erosion cases in Figure 1a—according to field observations—are qualified as “moderate or serious” erosion levels when the Van Schalkwyk method is applied. In Figure 1b, the Annandale method identifies some cases as scour when field observations find no scour. Finally, the Pells methods (Figure 1c,d) show some overlap among the observed and theoretical erosion classes.

The source of these inconsistencies could stem from either the rock mass resistance index or energy dissipation index, the latter representing the erosive force of water. The primary source of this inconsistency arises from incomplete observations of the erosion process. Indeed, since these data were obtained from laboratory tests using scaled-down physical models, they do not permit a comprehensive evaluation of the erosion process in rock masses [25,26]. Moreover, Boumaiza et al. evaluated the representativeness of various geomechanical parameters used in rock mass resistance indices [27,28]. They concluded that the various indices rely on some geomechanical parameters that are not relevant to hydraulic erosion when defining rock mass resistance. However, the observed inconsistency (e.g., Figure 1) could also stem from the erroneous assessment of the water erosive force, which is the focus of this paper.

Apart from the use of energy dissipation to represent the erosive force of water in many erosion-assessment methods, the average flow velocity (\bar{u} in $m \cdot s^{-1}$) and shear stress applied at the bottom of the flow channel ($\bar{\tau}_b$ in kPa) were identified as relevant for representing the water erosive force. These indices can be estimated using Equations (5) and (6). However, much criticism in regard to \bar{u} and the complexity of estimating $\bar{\tau}_b$ have discouraged their use in erosion-assessment methods.

$$\bar{\tau}_b = \rho \cdot g \cdot R_H \cdot S_f \cos \theta, \tag{5}$$

$$\bar{u} = \frac{1}{n} R_H^{2/3} S^{1/2}; \text{ where } n = \frac{R_H^{1/6}}{C} = R_H^{1/6} \sqrt{\frac{f}{8g}}, \tag{6}$$

where n is the Manning resistance coefficient, R_H is the hydraulic radius (m), S is the slope of the channel equal to dz/dx , x is the distance along the channel (m), z is the elevation above a datum (m), θ is the angle of inclination of the channel ($^\circ$), f is the Darcy [3,29] flow resistance coefficient, C is the Chézy [3,29] resistance coefficient, and S_f is the total energy gradient.

Moreover, the erosive force of water varies depending on the hydraulic conditions, including the water flow rate, the flow velocity, and the configuration of the spillway flow channel (Figure 2); thus, estimates of the erosive force can be affected by the problem of non-uniqueness. In Figure 2, four hydraulic conditions, A, B, C, and D, are presented. In conditions A and B, \bar{u} is set at $7 \text{ m}\cdot\text{s}^{-1}$, although the hydraulic conditions (flow rate and turbulence) in condition A are five times greater than those in B. Likewise, it is also apparent in Figure 2 that a single measure of the average shear stress or energy dissipation is not associated with a single particular condition of flow rate and hydraulic head. For example, the erosive force in conditions C and D may not be equivalent, even though the energy dissipation is constant [3].

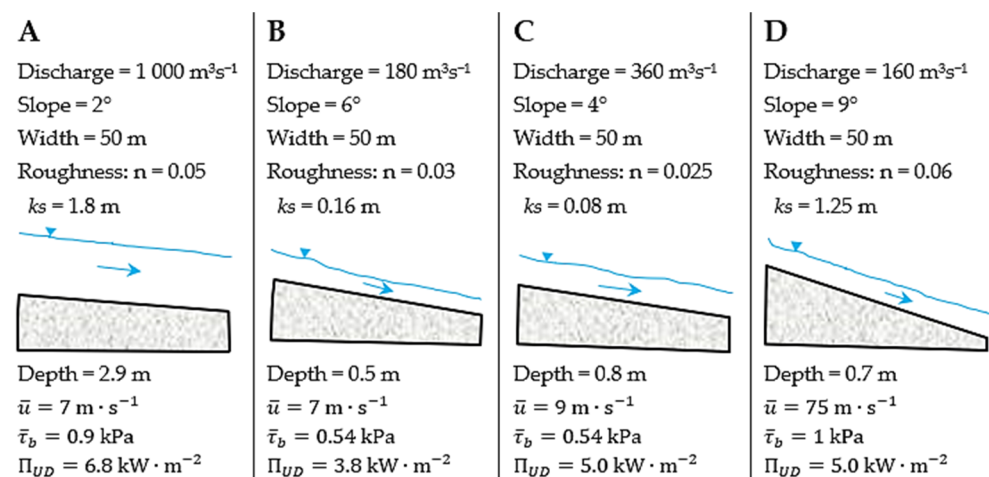


Figure 2. Examples of estimates when applying the different indices used to represent the erosive force of water.

In Figure 2, we note that \bar{u} , $\bar{\tau}_b$, and Π_{UD} can be affected by the problem of non-uniqueness, which can produce an under- or overestimate of the erosive force of the water. The average flow velocity represents a characteristic parameter of flow in the channel. This parameter is related to the channel slope and the hydrostatic force of the water in the dam reservoir. The average shear stress of the flow channel results from the normal stress applied to the bottom of the flow channel and represents an important component of the hydraulic erosion process. In terms of energy dissipation, this parameter correlates with the turbulence intensity of the flow [21,22]. Otherwise, few laboratory studies show a correlation between \bar{u} , $\bar{\tau}_b$, and Π_{UD} and the magnitude of pressure fluctuations in a flow channel. Thus, these different parameters have the same utility for representing the erosive force of water. The question arises of why there is the use of Π_{UD} rather than \bar{u} and $\bar{\tau}_b$ to represent the erosive force. According to the literature, the following apply:

- The non-representativeness of \bar{u} is linked to its sensitivity to the problem of non-uniqueness in the erosion process [3].
- The non-representativeness of $\bar{\tau}_b$ is linked to its complexity for estimating all probable mechanisms of erosion, including erosion by the dynamic expulsion of rock blocks and the erosion by the fragile failure of the rock mass into smaller pieces because of turbulent flow, a basic physical mechanism of erosion [30].

However, Π_{UD} , which is used by various erosion-assessment methods, is not always reliable because it does not integrate all the complexities of erosion; it is used to represent water erosive force because of its simplicity, not because of its representativeness. Thus,

the selection of Π_{UD} to represent the erosive force is based on a general qualitative analysis. This led Pells [3] to state that the recommendation for using Π_{UD} is pragmatic and concessional but not optimal.

Therefore, the determination of the best parameters to represent the erosive force of water is not based on sound analysis, and the justifications for rejecting some parameters, such as \bar{u} and $\bar{\tau}_b$, are qualitative. Hence, there is a need to verify the applicability of these different parameters to actual observed erosion data. In this context, we present a method to assess the applicability of the various and presumably relevant hydraulic parameters to represent the erosive force of water; these parameters include \bar{u} , $\bar{\tau}_b$, Π_{UD} , and the pressure head (h_u). We first describe the steps of our approach. We then apply our methodology to 100 observed cases of erosion within dam spillways. Finally, we identify the most relevant hydraulic parameters for quantifying the water erosive force within dam spillways.

2. Methods

We evaluate various hydraulic parameters in terms of their representativeness of erosive force. This approach is structured as (i) the identification of the hydraulic index or parameters used to represent the erosive force; (ii) compilation of a data set; (iii) data set analysis; and (iv) the visualization of correlations between the selected indices and erosion damage classes.

2.1. Erosive Force Index or Parameter

Π_{UD} , \bar{u} , and $\bar{\tau}_b$ were already identified as the relevant hydraulic indices for representing the erosive force of water; they were retained in order to validate their relevance.

Pressure applied within the rock mass discontinuities is a crucial hydraulic parameter causing erosion in multiple erosion mechanisms [31]. Figure 3 illustrates the removal of blocks; this removal is caused by the water pressure within the joints of a fractured rock mass and depends on the amplitude of fluctuating pressure within a turbulent flow. These fluctuations affect the pressure applied within the rock joints and increase the pressure force (F_u) directly below the rock blocks. The rock mass is then eroded by the dynamic expulsion of the blocks when the lifting pressure under the block exceeds the load resistance of the block. The parameters influencing the resistance of the block are the submerged weight of the block (G_b), the pressure forces on top of the block (F_o), and the shear resistance forces along the sides of the block (F_{sh}).

The hydraulic pressure depends on the flow velocity (dynamic pressure) and the head or static pressure (h_u). The head pressure is the only hydraulic parameter that depends on varying flow conditions (Figure 2). In Figure 2, the head pressure exerted on the bottom of the flow channel is the only parameter among \bar{u} , $\bar{\tau}_b$, and Π_{UD} that reflects the difference between the various hydraulic conditions. In conditions A and B, \bar{u} remains constant despite different flow rates and channel slopes; therefore, the erosive force would be the same, although the volume of water in condition A is five times greater than that in condition B. Similar observations can be made for $\bar{\tau}_b$ in conditions B and C and for Π_{UD} in conditions C and D. For each of these hydraulic conditions, however, the hydraulic pressure is a different value. As a result, the erosive force of the water differs among the conditions (A, B, C, and D) under the effect of the variable pressure head, which is equal to the depth of the water in the channel. Nevertheless, hydraulic pressure has never been studied deeply as a valid representative parameter for the erosive force of water. Moreover, to determine block uplift pressure, flow velocity and the head pressure in the rock mass joints must be known. However, no analytical methods or laboratory tests exist for estimating the flow velocity in a rock mass joint. For our approach, we consider the flow velocity in the channel as being representative or proportional to this velocity. The total pressure represented by two components (\bar{u} and h_u) is evaluated individually in this approach (Equations (6) and (7)).

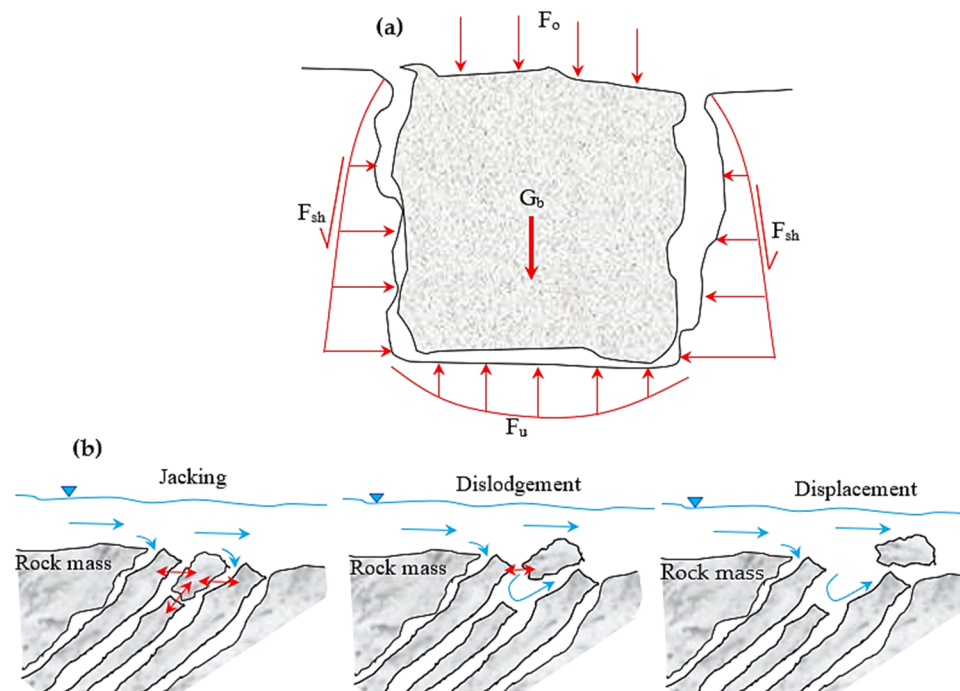


Figure 3. Erosion by block removal, named the dynamic block impulses, via (a) the removal of blocks in a plunging stream [16,32] and (b) the removal of blocks in a flow parallel to the bottom of the flow channel [21].

$$h_u = \frac{q}{u} = \frac{\text{m}^2/\text{s}}{\text{m}/\text{s}} = \text{water depth in m.} \quad (7)$$

Moreover, it is noteworthy that erosion process often varies because of the flow mode active at the spillways, with flow that is either plunging or parallel to the bed of the spillway [31]. The erosion processes commonly described in the literature are removal of blocks, brittle fracturing of the rock mass, and the fragile fracturing or fatigue erosion [16,32]. Based on the analysis of these erosion processes (Figure 2), it becomes apparent that the underlying mechanism of erosion in different process is very similar, and the pressure exerted within the rock mass and its discontinuities emerges as the causal parameter of erosion, which is tested in this paper.

2.2. Data Set Development

The data set includes observational data from several dam spillways that have experienced erosion. This data set includes multiple geomechanical and hydraulic parameters related to the erosional process, allowing us to estimate various parameters in Equations (4)–(7). These data come from compilations of erosion cases observed at several dam spillways in South Africa [20] and Australia [3], which are characterized by distinct geographical and geological conditions. These data are available in Appendixes C and D of Pells' thesis. Note that the data points in Figure 1b–d originate from this case study data set.

2.3. Data Analysis Methods

The first step of this analysis consists of categorizing the data set into classes defined by a rock mass resistance index; for example, the *eGSI* categories rock mass in to very poor, poor, moderate, good, and very good rock mass quality (Table 2).

Subsequently, each rock mass class is arranged in terms of damage (Table 3), which may be negligible, minor, moderate, large, or extensive. Erosion classes are defined by the depth (m) or quantity (m^3 per 100 m^2) of eroded rock mass [3,23].

Table 2. Rock mass class according to *eGSI*, derived from the GSI of Hoek [24].

Rock Mass Class (<i>eGSI</i>)		
1	Very poor	<20
2	Poor	21–40
3	Moderate	41–60
4	Good	61–80
5	Very good	81–100

Table 3. Erosion classes as defined by Pells [3,23].

Max Depth (m)	General Extent m ³ per 100 m ²	Class	Descriptor
<0.3	<10	I	Negligible
0.3–1	10–30	II	Minor
1–2	30–100	III	Moderate
2–7	100–350	IV	Large
>7	>350	V	Extensive

The mean value of each index of the erosive force of water and rock mass resistance is calculated using Equation (8), per erosion damage classes, and depending on the rock mass quality class.

$$\bar{In}_{(EC/RMC)} = \frac{\sum(In_1 + In_2 + \dots + In_N)}{N} \tag{8}$$

where $\bar{In}_{(EC/RMC)}$ is the mean value of the index (erosive force or resistance of the rock mass) of the erosion class (EC) per rock mass class (RMC), *In* is the index for each erosion case by erosion class, and *N* is the number of erosion cases per erosion class.

Table 4 illustrates how Class 2 of the *eGSI* rock mass index is determined, and Table 5 presents the calculation performed for all classes of the *eGSI* rock mass index in relation to \bar{u} . Then, Table 5 is prepared for each parameter or index of water erosive force coupled to different rock mass indices.

Table 4. Summary of the calculation applied to the parameters \bar{u} and *eGSI* for Class 2 of the *eGSI* index.

Rock Mass Index Class <i>eGSI</i>		Peak \bar{u} (m·s ⁻¹)	Dam ID	Erosion Level	\bar{eGSI}	\bar{u}
Class 2 21 < <i>eGSI</i> < 40	25	13.3	Cop.6	Extensive	27	17
	25	21.2	Cop.10			
	32	15.5	Cop.5			
	32	10.1	Pin.4	Large	34	16
	32	12	Cop.4			
	32	18.8	Cop.9			
	40	25	Bur.4			
	23	6.8	Kli.2	Minor	27	11
	23	7.2	Kli.5			
	23	12.6	Gar.2			
	23	15.1	Gar.5			
	32	9.1	Kam.5			
	35	12.2	Cop.11	Moderate	31	11
	23	8.5	Kli.3			
	31	15.6	Goe.2			
	31	15.6	Goe.4			
	31	12.3	Goe.5			
	31	13.2	Hart.2			
31	10	Kam.3				
31	5.1	Pin.2				
32	14.5	Cop.7	Negligible	25	6	
35	6.8	Cop.1				
25	5.2	Gar.1	Negligible	25	6	
25	6.8	Gar.4				

Table 5. Summary of the calculation applied to the parameters \bar{u} and $eGSI$.

Rock Mass Class According to $eGSI$			Erosion Class									
			Negligible		Minor		Moderate		Large		Extensive	
			\bar{u}	$eGSI$	\bar{u}	$eGSI$	\bar{u}	$eGSI$	\bar{u}	$eGSI$	\bar{u}	$eGSI$
1	Very poor	<20	–	–	–	–	9	9	10	10	20	11
2	Poor	21–40	6	25	11	27	11	31	16	34	17	27
3	Moderate	41–60	4	46	6	51	11	50	10	55	–	–
4	Good	61–80	9	70	11	70	15	69	22	72	–	–
5	Very good	81–100	–	–	–	–	–	–	–	–	–	–

Note: (–) indicates the absence of erosion data for these classes of rock mass.

2.4. Presentation of the Results Obtained in Graphic Form

The data obtained in tabular form—12 tables similar to Table 5—are represented graphically. The graphs constructed for each pair of hydraulic erosion evaluation parameters or indices, e.g., \bar{u} vs. K , \bar{u} vs. $eGSI$, and \bar{u} vs. $RMEI_B$, are characterized by regression lines representing the erosion classes.

To ensure that our classes are truly representative, we only consider the damage classes having a minimum of three points, i.e., having characterizing data for a minimum of three rock mass classes, when visualizing the results in graph form. Finally, it is expected that the most relevant pair indices will correlate well with erosion class.

3. Results and Discussions

The above-described approach aims to assess the relevance of various water erosive force parameters. We obtained 12 graphs by comparing each index or parameter of the erosive force of the water with a rock mass resistance index. For the interpretation of these graphs, we consider (i) the correlation to be reliable when a logical sequence is respected following erosion damage classes. A logical sequence means that the regression lines passing through the observed erosion cases permit differentiating the erosion classes according to erosion damage, i.e., the regression lines of the damage classes must have a different and increasing slope with greater erosion damage, and (ii) the representativeness of the regressions lines is also considered, as regression lines having a higher R^2 are deemed more reliable.

3.1. \bar{u} as a Function of Rock Mass Resistance Index

Using the average flow velocity (\bar{u})—the first component of hydraulic pressure—to represent the erosive force of water, we can plot the observed erosion damage against the various rock mass indices (K , $eGSI$, and $RMEI_B$) (Figure 4).

The regression lines allow a further differentiation of the erosion classes (Figure 4). Regression lines for \bar{u} and the K and $RMEI_B$ indices (Figure 4a,b) illustrate an incongruence among the damage classes, i.e., the regression lines do not differentiate the erosion damage classes. However, we can differentiate the different erosion damage classes when \bar{u} is compared with the $eGSI$ rock mass index (Figure 4c). The regression lines in the latter case do not cross with greater slopes as the severity of damage increases (negligible to large damage).

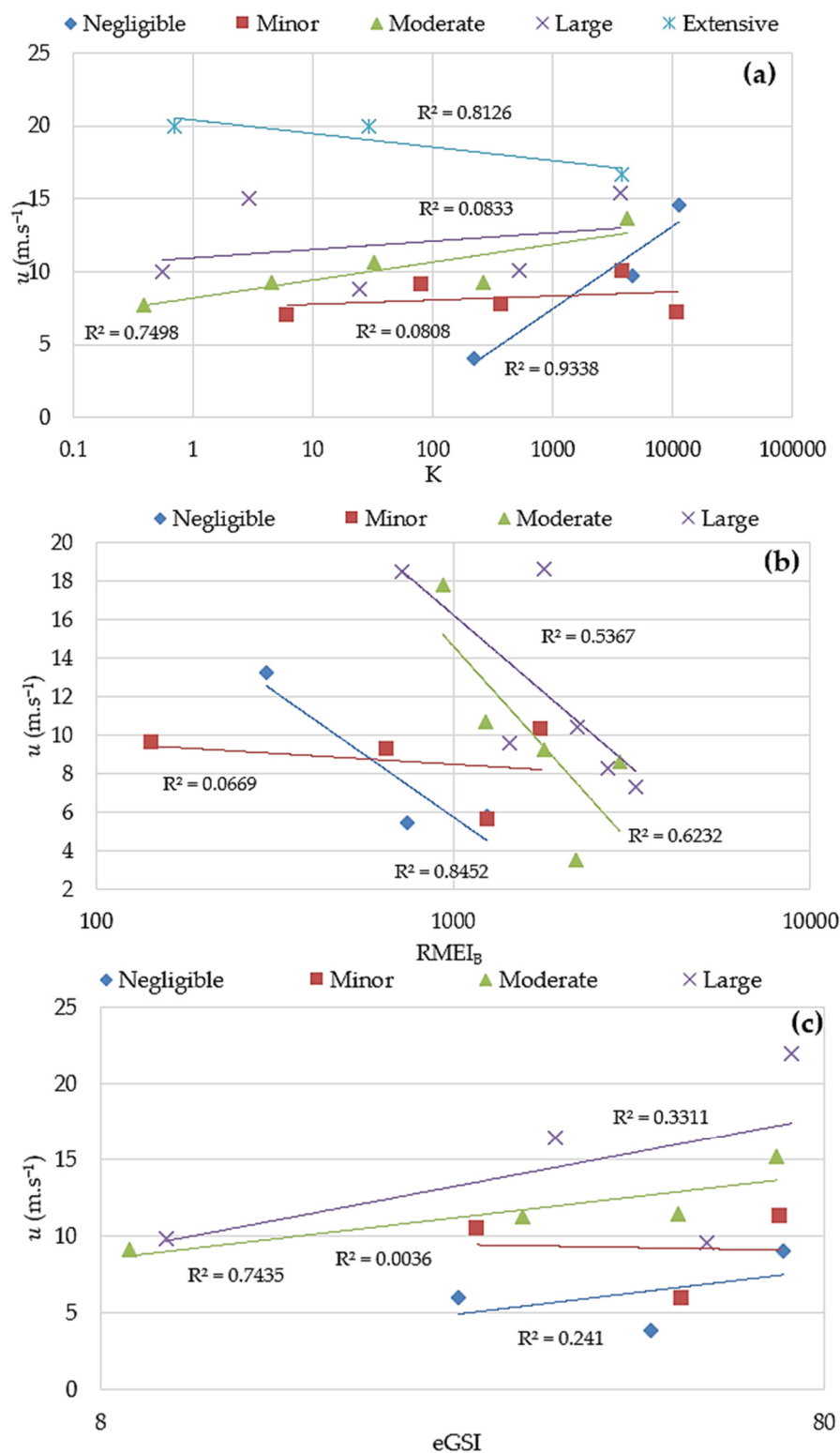


Figure 4. Observed erosion damage plotted using \bar{u} as the erosive force of water vs. rock mass resistance indices; (a) K , (b) $RMEI_B$, and (c) $eGSI$.

3.2. τ_b as a Function of Rock Mass Resistance Index

Using the shear stress of the bottom of the flow channel (τ_b) to represent the erosive force of the water, we can plot the considered erosion damage class against the rock mass resistance indices (Figure 5).

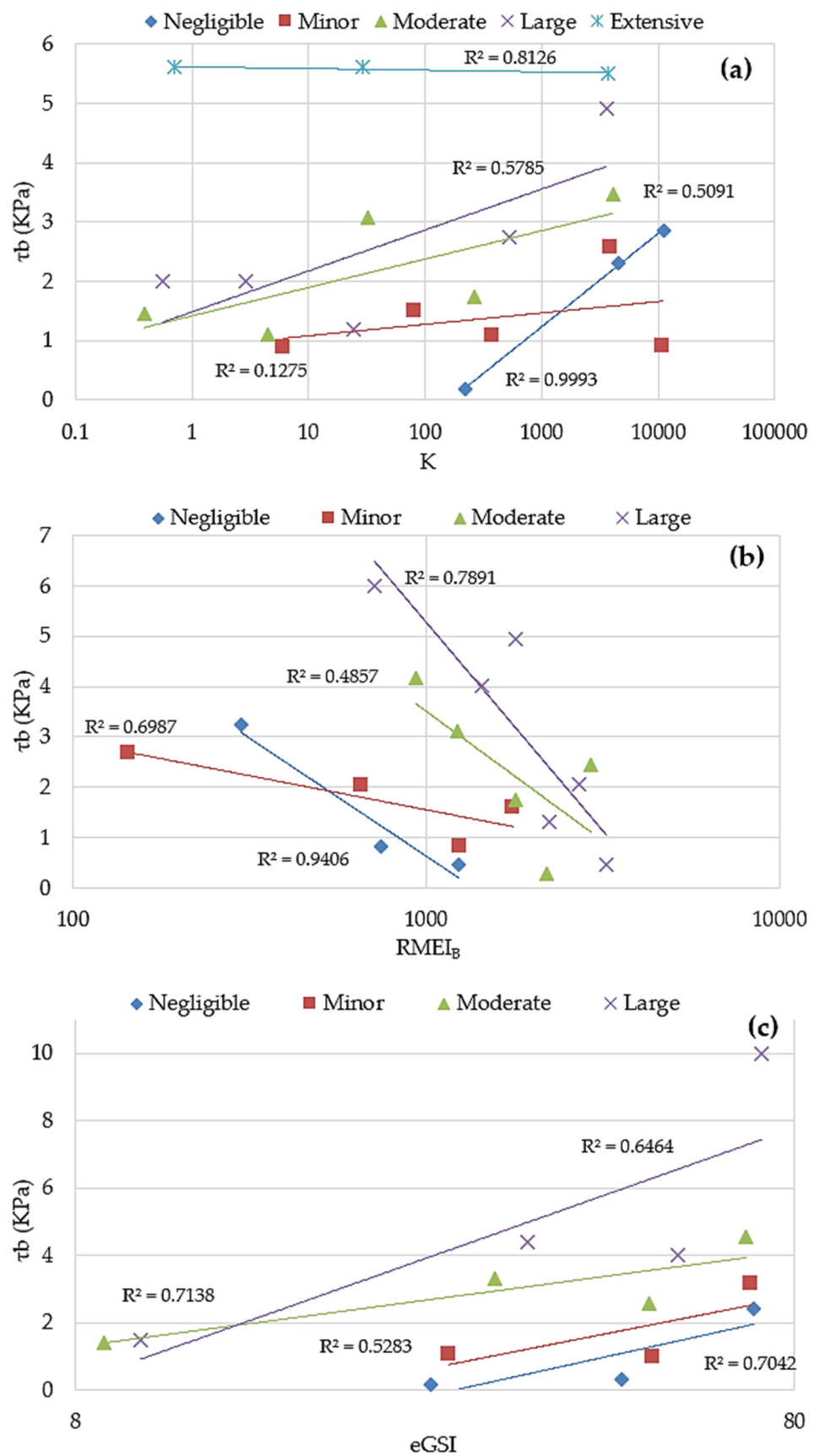


Figure 5. Observed erosion damage plotted using τ_b as the erosive force of water vs. rock mass resistance indices; (a) K , (b) $RMEI_B$, and (c) $eGSI$.

Only the plot of τ_b vs. $eGSI$ presents regression lines showing some logical sequence among the various erosion classes, as regression lines cross for τ_b vs. $RMEI_B$ and τ_b vs. K . For the τ_b vs. $eGSI$ graph (Figure 5c), the negligible, minor, and moderate damage classes follow an expected logical sequence; however, this pattern is disturbed by the large damage class regression line that intersects the moderate damage class. Thus, τ_b correlates less well with observed erosion damage classes than \bar{u} .

3.3. Π_{UD} as a Function of Rock Mass Resistance Index

When we use the dissipation of energy (Π_{UD}) to represent the erosive force, no clear pattern are observed among the various erosion damage classes (Figure 6). Thus, use of energy dissipation to represent the erosive force of water is not optimal because it does not correlate with the observed erosion damage classes.

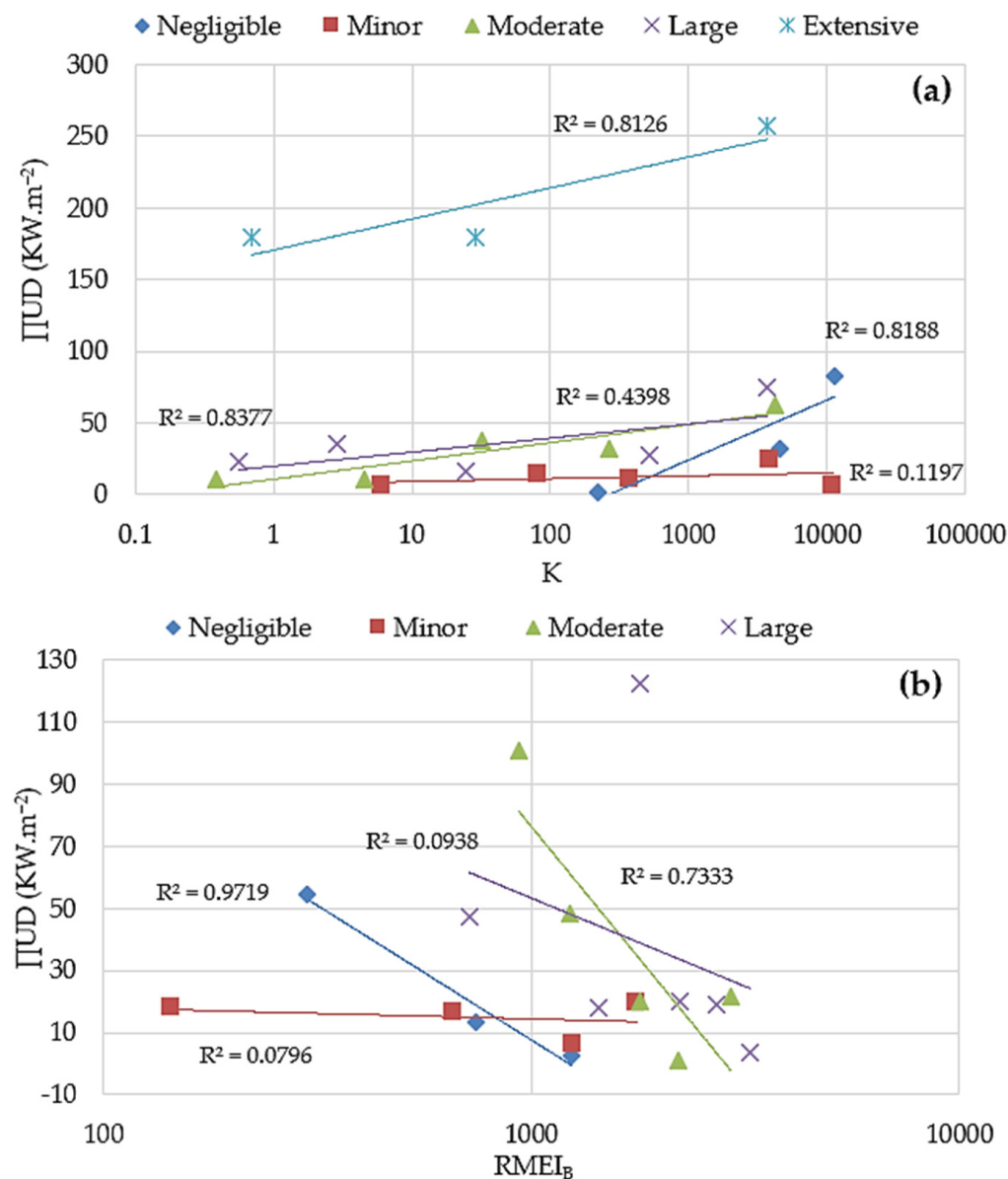


Figure 6. Cont.

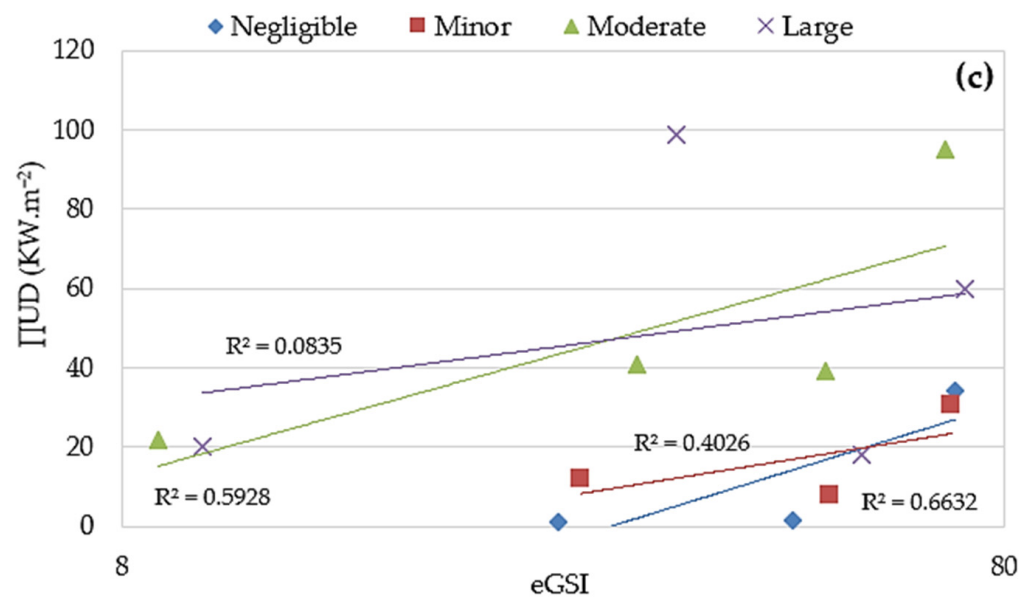


Figure 6. Observed erosion damage plotted using Π_{UD} as the intensity of the erosive force of water vs. rock mass resistance indices; (a) K , (b) $eGSI$, and (c) $RMEI_B$.

3.4. h_u as a Function of Rock Mass Resistance Index

When we use the pressure head, the second component of hydraulic pressure, as a function of the various rock mass resistance indices (Figure 7), patterns that are nearly identical to those of \bar{u} representing the erosive force are observed.

Plots of h_u versus $RMEI_B$ and K do not produce a logical pattern of regression lines of erosion damage class (Figure 7a,b); however, we can observe a logical sequence of regression lines for h_u vs. $eGSI$.

Using these graphs, the relevance of each water erosive force parameter is summarized in Table 6.

Table 6. Evaluation of the representativeness of the different indices. The R^2 value represents the average R^2 of all regression lines.

Methods	Logical Sequence	R^2
\bar{u} vs. K	No	0.53
\bar{u} vs. $eGSI$	Yes	0.32
\bar{u} vs. $RMEI_B$	No	0.52
τ_b vs. K	No	0.60
τ_b vs. $eGSI$	No	0.65
τ_b vs. $RMEI_B$	No	0.72
Π_{UD} vs. K	No	0.61
Π_{UD} vs. $eGSI$	No	0.43
Π_{UD} vs. $RMEI_B$	No	0.47
h_u vs. K	No	0.49
h_u vs. $eGSI$	Yes	0.60
h_u vs. $RMEI_B$	No	0.31

It was expected that the most relevant parameter of the erosive force of water, when compared with a rock mass resistance index, would show a logical sequence between the different classes of erosion with less variability. A logical pattern for the damage classes is obtained only when head pressure (h_u) and velocity (\bar{u}) are plotted against $eGSI$. The other indices, energy dissipation (Π_{UD}) and shear stress ($\bar{\tau}_b$), do not present a logical sequence with respect to damage classes. It appears that Π_{UD} is the least relevant parameter for representing the erosive force of water because the regression lines of the damage classes do not present any logical trend. The $\bar{\tau}_b$, on the other hand, presents a certain logic for

the three least severe damage classes but not for all the damage classes, which makes it irrelevant.

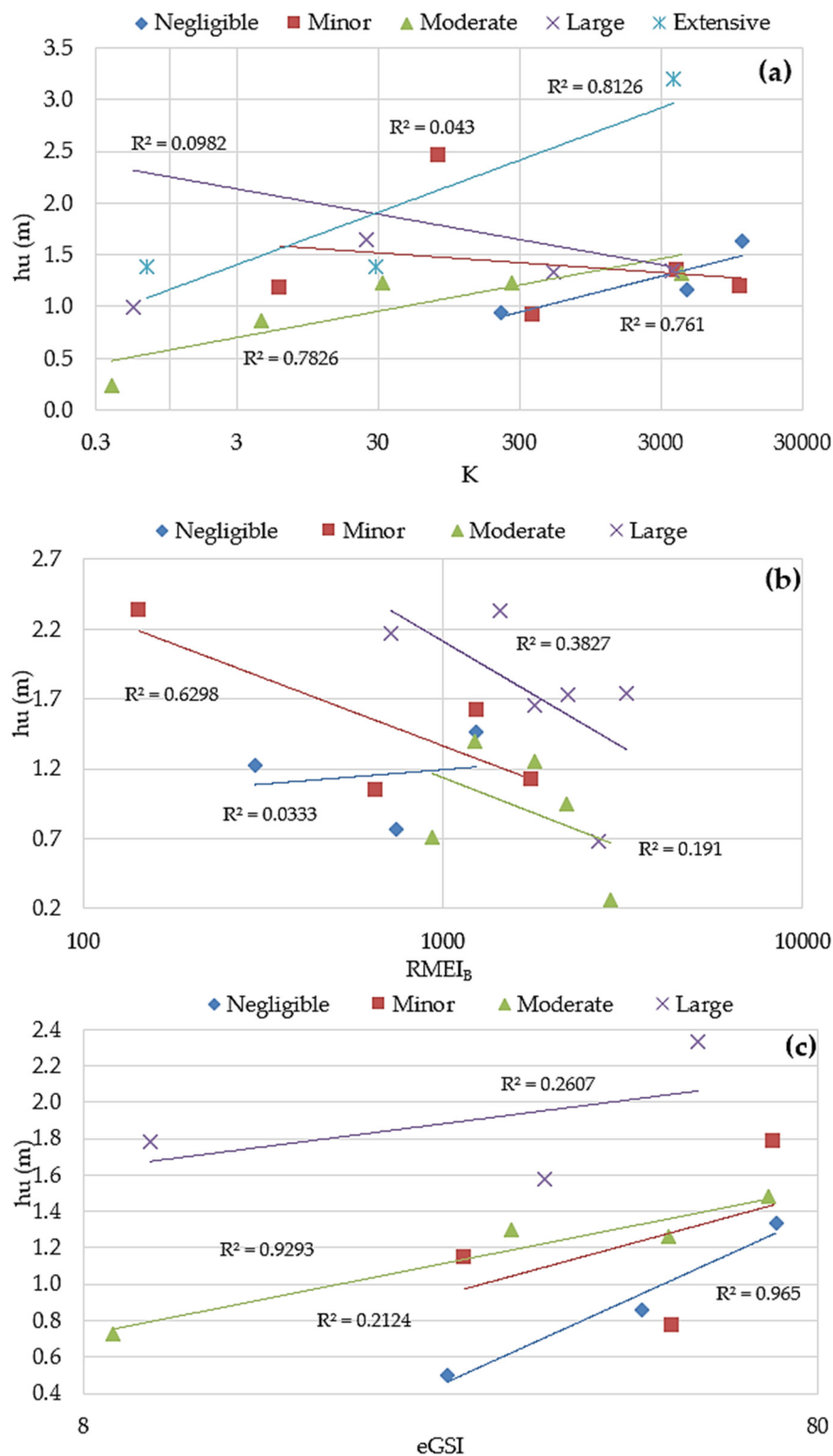


Figure 7. Observed erosion damage plotted using h_u as the intensity of the erosive force of water vs. the rock mass resistance indices; (a) K , (b) $eGSI$, and (c) $RMEI_B$.

A logical relationship among the damage classes is obtained only using h_u or \bar{u} to represent the erosive force of water. This result agrees with the existing understanding

of erosion mechanisms. According to this, the hydraulic pressure applied within the discontinuities of the rock mass is the main parameter underlying erosion [25,30,33]. The hydraulic pressure in spillways is directly linked to h_u and \bar{u} , which represent the two components of pressure—static pressure relates to water height in the channel, and dynamic pressure relates to flow velocity; it is entirely plausible that these parameters correlate with the damage scale of spillways. However, \bar{u} is a little bit affected by a problem of non-uniqueness because the distribution of the plotted erosion cases is quite variable ($R^2 < 0.5$). This variability in the dynamic component of the pressure could be explained by the fact that the behavior of the dynamic pressure would be different from that in the rock mass discontinuities. It should be noted that the desired pic pressure is applied in the rock mass discontinuities.

For the various known erosion mechanisms, the hydraulic pressure applied to the rock mass seems to be the triggering factor of erosion. Therefore, future research should be directed toward estimating this pressure applied to the discontinuities of a rock mass. An estimate of this pressure requires the missing parameter, which is the flow velocity in the rock mass joints. For this, laboratory studies can provide a promising base for future research [28,32]. The laboratory spillway model can allow for estimating flow velocity in the discontinuities of a rock mass [25]. By knowing the flow velocity within the channel and joints, a correlation factor between this pair of velocities can be determined in relation to the condition of the rock mass. Furthermore, it emerges from this analysis that *eGSI* seems to be the most reliable index of the rock mass quality in the hydraulic erosion domain.

The results obtained from this analysis prove to be relevant because, based on real case data of erosion, the key parameters to look for to better estimate the erosive force of water are identified. However, it should be noted that these results could be affected by the limited quantity of data available. However, it should be remembered that the majority of methods for evaluating hydraulic erosion of spillways (Figure 1) were developed using the same data. Future research in this field should include the acquisition of new data to enhance this database. A practical and cost-effective approach involves conducting experimental tests using scaled-down physical laboratory models that offer greater representativeness [24,32].

4. Conclusions

The analysis approach presented was conducted on data collected from more than 100 cases of spillway erosion to determine the applicability of several indices of erosive force. It emerges from analysis that (i) energy dissipation is not the ideal index to represent the erosive force of water; and (ii) hydraulic pressure appears to be the best-suited for representing the erosive force of water. This study underlines the importance of developing a means of estimating the total pressure within rock mass joints. This necessarily involves determining the water depth in the spillway channel, a component determining the static pressure, and estimating flow velocity within the rock mass joints, a component linked to dynamic pressure.

Given the importance of spillways in hydraulic installations, additional data on spillways erosion should be research. Thus, future work needs to obtain a greater amount of on-site erosion data that need to be combined with laboratory-scale experiments and numerical modeling to develop a comprehensive method for assessing the stability of these structures.

Author Contributions: Conceptualization, A.S.K.; methodology, A.S.K. and A.S.; software, A.S.K.; validation, A.S.K., A.S., A.R. and M.Q.; formal analysis, A.S.K.; investigation, A.S.K.; resources, A.S.K. and A.S.; writing—original draft preparation, A.S.K.; writing—review and editing, A.S.K., A.S., A.R. and M.Q.; visualization, A.S.K., A.S., A.R. and M.Q.; supervision, A.S., A.R. and M.Q.; project administration, A.S., A.R. and M.Q.; funding acquisition, A.S. All authors have read and agreed to the published version of the manuscript.

Funding: Natural Sciences and Engineering Research Council of Canada (NSERC) and Hydro-Québec for funding through the RDC program (RDC 537350).

Data Availability Statement: All data, models, and code generated or used during the study appear in the submitted article.

Conflicts of Interest: Author Marco Quirion was employed by the company Hydro-Québec. The remaining authors declare that the research was conducted in the absence of any commercial or financial relationships that could be construed as a potential conflict of interest.

Abbreviations

The following symbols are used in this paper:

B_f	Channel width (m).
C	Chezy's flow resistance coefficient.
eGSI	Geological force index for erodibility.
f	Darcy's flow resistance coefficient.
GSI	Geological strength index.
g	Gravitational acceleration (m s^{-2}).
HEC-RAS	Hydrologic engineering centers river analysis system
J_s/E_{doa}	Relative structure of the block.
K	Kirsten index.
K_b	Rock block size.
K_d	Shear strength of the rock mass joints.
M_s	Confined compressive strength of the intact rock.
n	Manning resistance coefficient.
Q	Water flow rate ($\text{m}^3 \text{s}^{-1}$).
q	Flow rate per unit length of channel width ($\text{m}^2 \text{s}^{-1}$).
R_H	Hydraulic radius (m).
RMEI_B	Rock mass erodibility index.
S	Flow channel slope.
S_f	Total energy gradient.
\bar{u}	Average velocity (m s^{-1}).
V_b	Block volume (m^3).
θ	Channel's angle of inclination ($^\circ$).
ρ	Water density (kg m^{-3}).

References

- Alvi Associates, Inc. *Case Study: Oroville Dam (California, 2017)*; Alvi Associates, Inc.: Towson, MD, USA, 2023.
- Alvi, I.A.; Alvi, I.S. Why dams fail: A systems perspective and case study. *Civ. Eng. Environ. Syst.* **2023**, *40*, 150–175. [[CrossRef](#)]
- Pells, S.E.; Pells, P.J.; Peirson, W.L.; Douglas, K.; Fell, R. *Erosion of Rock in Spillways*; University of New South Wales: Kensington, Australia, 2016.
- Withers, W.J. *Pressure Fluctuations in the Plunge Pool of an Impinging Jet Spillway*; University of Glasgow: Glasgow, Scotland, 1991.
- Manso, P.F.d.A.; Schleiss, A. *The Influence of Pool Geometry and Induced Flow Patterns in Rock Scour by High-Velocity Plunging Jets*; EPFL (Lausanne): Lausanne, Switzerland, 2006.
- Lesleighter, E.J.; Bollaert, E.F.R.; McPherson, B.L.; Scriven, D.C. Spillway Rock Scour Analysis—Composite of Physical & Numerical Modelling, Paradise Dam, Australia. In Proceedings of the 6th IAHR International Symposium on Hydraulic Structures, Portland, OR, USA, 27–30 June 2016; pp. 343–352.
- Gu, S.; Ren, L.; Wang, X.; Xie, H.; Huang, Y.; Wei, J.; Shao, S. SPHysics Simulation of Experimental Spillway Hydraulics. *Water* **2017**, *9*, 973. [[CrossRef](#)]
- Kote, A.S.; Nangare, P.B. Hydraulic Model Investigation on Stepped Spillway's Plain and Slotted Roller Bucket. *Eng. Technol. Appl. Sci. Res.* **2019**, *9*, 4419–4422. [[CrossRef](#)]
- Sawadogo, O. *Scour of Unlined Dam Spillways*; Stellenbosch University: Stellenbosch, South Africa, 2010.
- Tuna, M.C. Effect of offtake channel base angle of stepped spillway on scour hole. *Iran. J. Sci. Technol. Trans. Civ. Eng.* **2012**, *36*, 239–251.
- Wilkinson, C.; Harbor, D.J.; Helgans, E.; Kuehner, J.P. Plucking phenomena in nonuniform flow. *Geosphere* **2018**, *14*, 2157–2170. [[CrossRef](#)]
- Montgomery, R.A. *Investigations into Rock Erosion by High Velocity Water Flows*; Royal Institute of Technology: Stockholm, Sweden, 1984.
- Reinius, E. Rock erosion. *Int. Water Power Dam Constr.* **1986**, *38*, 43–48.
- Annandale, G.; Wittler, R.; Ruff, J.; Lewis, T. Prototype validation of erodibility index for scour in fractured rock media. In Proceedings of the International Water Resources Engineering Conference, Memphis, TN, USA, 3–7 August 1998; pp. 1096–1101.

15. Liu, P.Q.; Dong, J.R.; Yu, C. Experimental investigation of fluctuation uplift on rock blocks at the bottom of the scour pool downstream of Three-Gorges spillway. *J. Hydraul. Res.* **1998**, *36*, 55–68. [[CrossRef](#)]
16. Bollaert, E.; Schleiss, A. *Transient Water Pressures in Joints and Formation of Rock Scour Due to High-Velocity Jet Impact*; EPFL-LCH: Lausanne, Switzerland, 2002.
17. Wang, Y.-K.; Jiang, C.-B. Experimental study of drag reduction in flumes and spillway tunnels. *Water Sci. Eng.* **2010**, *3*, 200–207.
18. George, M.; Sitar, N.; Sklar, L. Experimental evaluation of rock erosion in spillway channels. In Proceedings of the 49th US Rock Mechanics/Geomechanics Symposium, San Francisco, CA, USA, 29 June–1 July 2015.
19. Moore, J.S.; Temple, D.M.; Kirsten, H.A.D. Headcut advance threshold in earth spillways. *Bull. Assoc. Eng. Geol.* **1994**, *31*, 2.
20. Van Schalkwyk, A.; Jordaan, J.; Dooge, N. Erosion of rock in unlined spillways. *Int. Comm. Large Dams* **1994**, *71*, 555–571.
21. Annandale, G. Erodibility. *J. Hydraul. Res.* **1995**, *33*, 471–494. [[CrossRef](#)]
22. Kirsten, H.A.; Moore, J.S.; Kirsten, L.H.; Temple, D.M. Erodibility criterion for auxiliary spillways of dams. *Int. J. Sediment Res.* **2000**, *15*, 93–107.
23. Pells, S.E.; Douglas, K.; Pells, P.J.N.; Fell, R.; Peirson, W.L. Rock Mass Erodibility. *J. Hydraul. Eng.* **2017**, *143*, 06016031. [[CrossRef](#)]
24. Hoek, E.; Marinos, P.; Benissi, M. Applicability of the Geological Strength Index (GSI) classification for very weak and sheared rock masses. The case of the Athens Schist Formation. *Bull. Eng. Geol. Environ.* **1998**, *57*, 151–160. [[CrossRef](#)]
25. Koulibaly, A.S.; Saeidi, A.; Rouleau, A.; Quirion, M. A Reduced-Scale Physical Model of a Spillway to Evaluate the Hydraulic Erodibility of a Fractured Rock Mass. *Rock Mech. Rock Eng.* **2022**, *56*, 933–951. [[CrossRef](#)]
26. Wisse, M.-H.; Saeidi, A.; Quirion, M.; Nilsson, C.-O. Effects of joint opening and block protrusion on the hydraulic parameters affecting rock block erosion in unlined spillways using a reduced-scale model. *Acta Geotech.* **2023**, *19*, 1965–1979. [[CrossRef](#)]
27. Boumaiza, L.; Saeidi, A.; Quirion, M. A method to determine relevant geomechanical parameters for evaluating the hydraulic erodibility of rock. *J. Rock Mech. Geotech. Eng.* **2019**, *11*, 1004–1018. [[CrossRef](#)]
28. Boumaiza, L.; Saeidi, A.; Quirion, M. A method to determine the relative importance of geological parameters that control the hydraulic erodibility of rock. *Q. J. Eng. Geol. Hydrogeol.* **2021**, *54*, qjeh2020-154. [[CrossRef](#)]
29. Cengel, Y. *Heat and Mass Transfer: Fundamentals and Applications*; McGraw-Hill Higher Education: New York, NY, USA, 2014.
30. Bollaert, E.F.; Schleiss, A.J. Physically based model for evaluation of rock scour due to high-velocity jet impact. *J. Hydraul. Eng.* **2005**, *131*, 153–165. [[CrossRef](#)]
31. Koulibaly, A.S.; Saeidi, A.; Rouleau, A.; Quirion, M. Identification of hydraulic parameters influencing the hydraulic erodibility of spillway flow channels. *Water* **2021**, *13*, 2950. [[CrossRef](#)]
32. Annandale, G.W. Current Technology to Predict Scour of Rock. In Proceedings of the Golden Rocks 2006, the 41st U.S. Symposium on Rock Mechanics (USRMS), Golden, CO, USA, 17–21 June 2006; p. 11.
33. Koulibaly, A.S. *Conception d'un Modèle de Laboratoire d'un Évacuateur de crue pour Étudier L'érosion des Masses Rocheuses*; Université du Québec à Chicoutimi: Chicoutimi, QC, Canada, 2021.

Disclaimer/Publisher's Note: The statements, opinions and data contained in all publications are solely those of the individual author(s) and contributor(s) and not of MDPI and/or the editor(s). MDPI and/or the editor(s) disclaim responsibility for any injury to people or property resulting from any ideas, methods, instructions or products referred to in the content.